Iranian Journal of Electrical and Electronic Engineering

Journal Homepage: ijeee.iust.ac.ir

A Novel Multi-Port Converter for Photovoltaic Systems

Homa Zarei Zohdi*, Mohammad Sarvi*(C.A.) and Heidar Ali Shayanfar*

Abstract: In this paper, a novel multi-input converter for photovoltaic applications is introduced. The suggested topology has a single output and three input ports including: solar panel, fuel cell, and a bidirectional port for battery charging and discharging. The converter operates in three distinct modes, each defined by a specific duty cycle, allowing for precise adjustment of the output voltage and controlled power sharing between the sources. This configuration allows for independent management of the fuel cell, solar panel and battery ensuring efficient energy utilization under different generation and load conditions. One of the key advantages of the proposed converter is its continuous input current with very low ripple, which helps to extend the lifetime of the fuel cell and photovoltaic sources. This topology also achieves high voltage gain without bulky transformers, maintains high efficiency over a wide power range, and provides a common ground between all ports. These features reduce the voltage stress on the semiconductor switches and improve system reliability. The proposed converter is compared with recent multi-input converters and its advantages in component count, voltage suppression, control simplicity, and voltage gain are demonstrated. Simulation results for a 330 W sample in MATLAB/Simulink confirm proper output voltage regulation and satisfactory performance of the converter under various operating conditions.

Keywords: DC-DC Converter, Multi-input converter, Photovoltaic System, Voltage Gain.

In Press

1 Introduction

In recent years, the use of renewable resources, including photovoltaic (PV) systems, has increased significantly [1]-[2]. To solve the problem of the shortage of renewable resources and to ensure the supply of power, energy storage devices such as batteries and other energy sources such as fuel cells are used [3]-[4]. Hybrid systems require more than one converter to control the power, and the converter on the energy storage side must be bidirectional [5]. Power management with single converters is inefficient, and the system cost increases and the system is more bulky [6]. Therefore, multi-input (MI) converters can significantly contribute to the effective combination of multiple resources [7].

In [8] a multi-input-multi-output (MI-MO) converter was presented that is modular but not suitable for high-power applications and has high input source current ripple. The combination of a voltage multiplier cell and coupled inductors in the structure can increase the gain of the multiport converter [9]-[10].

In [11]-[12], a non-isolated converter architecture featuring three ports is presented.

In [13] a two-input-single-output converter with high input voltage gain was presented. In [14] presented an isolated multi-port converter, and since two transformers are used and the number of capacitors is large, the converter analysis is complex and its manufacturing cost is high. In [15] an isolated multiport converter for PV-battery configurations was presented. In [16] a non-isolated topology tailored for hybrid PV-battery applications is introduced.

Iranian Journal of Electrical & Electronic Engineering, 2027.
Paper first received 17 April 2026 and accepted 09 October 2026.
* The author is with the Department of Electrical Engineering, Iran University of Science and Technology, Tehran, Iran.
E-mails:msarvi@iust.ac.ir.
Corresponding Author: Mohammad Sarvi.

In [17], a three-port converter was presented with only one inductor, and due to the low energy storage, the converter is not stable in high-power applications. In [18] a DC-DC converter with multiple output ports was presented, with each output compatible with different devices.

In [19]-[20], a comprehensive review of the types of isolated and non-isolated multiport converter structures has been provided.

In [21], a multi-port converter is introduced that allows combining three input sources and is suitable for practical energy management applications.

In [22] multi-port converters for renewable sources are presented, and the large number of elements makes the implementation of the converter for industrial applications difficult and costly.

Considering the challenges discussed in the literature, in this study, a new bidirectional multi-input converter is introduced, which can use solar panel, battery and fuel cell simultaneously. The introduced converter demonstrates a favorable voltage-gain and efficiency characteristic. Continuous input current and common ground between ports are other features of the proposed structure. By comparing the proposed converter with other converters, the good performance and efficiency of the proposed converter have been validated.

This paper is structured into five sections. Section 2 is presented the structure of the proposed converter and its analysis. The third section compares the converter with other converters. The fourth section is provided the simulation of the converter and finally, the last part is presented the conclusion.

2 Converter Structure and Operating Modes

The general schematic of the multi-input photovoltaic system is shown in Fig. 1(a) and with the Suggested MI converter in Fig.1(b). According to the figure, in the latter case, the number of converters is reduced. Fig. 2 shows the Suggested MI DC-DC converter. The first operating mode is for when the load is powered by the solar panel and fuel cell. The second mode is for when the battery is in a discharged state and supplies the load together with the panel and fuel cell. The third mode occurs when the battery is charging and the load is supplied by the panel and fuel cell. This converter has 3 operating modes that are implemented by three duty cycles (d1, d2, d3).

The state of the semiconductor elements in each mode is summarized in Table 1.

2.1 First Mode of Operation

In this case, the solar panel and fuel cell supply the load. This mode has 3 switching states as shown in Fig. 3(a) to Fig. 3(c).

State 1 [t0, t1]: At this duration, switches S1, S5, S4 and diode D6 are on and capacitor C1 and inductors L1, L2 are charging.

The converter equation in this mode is as follows, and the current in inductor L1 is equal to i1 and the current in inductor L2 is equal to i2.

$$V_{c1} = L_1 \frac{di_1}{dt} \quad (1)$$

$$V_{pv} = V_{c1} \quad (2)$$

$$V_{FC} = L_2 \frac{di_2}{dt} \quad (3)$$

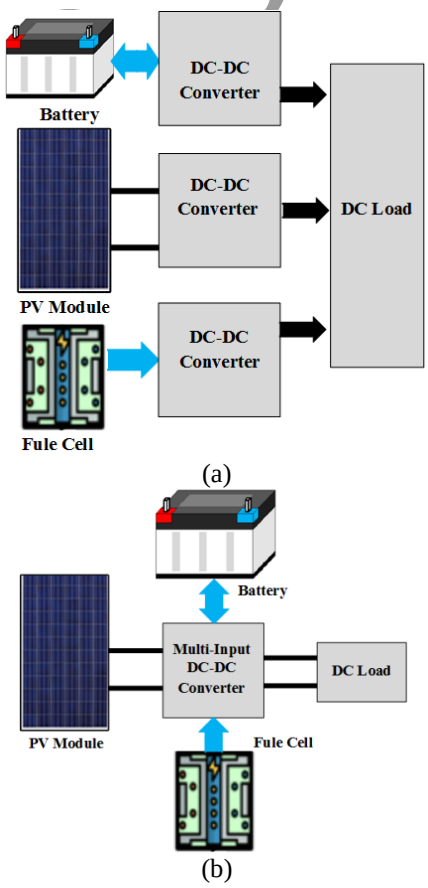


Fig 1. (a) System with separate converters, (b) System with MI converter.

In Press

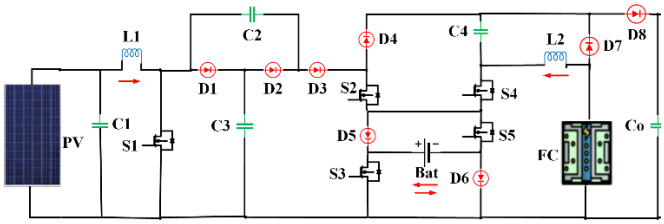


Fig 2. The Suggested MI converter.

State 2[t1, t2]: D1, D3, D4, D6 and D8 are on and inductor L1 is charging capacitor C4. Inductor L2 is charging and the output load is powered.

$$V_{c1} = L_1 \frac{di_1}{dt} + V_{c2} + V_{c4} \quad (4)$$

$$V_{FC} = L_2 \frac{di_2}{dt} \quad (5)$$

$$V_{c1} = L_1 \frac{di_1}{dt} + V_{c2} + V_{co} \quad (6)$$

$$V_{c1} = L_1 \frac{di_1}{dt} + V_{c3} \quad (7)$$

State 3 [t2, t3]: At t=t2, diode D8 is on and the output load is powered (Fig. 3 (c)).

$$V_{FC} = L_2 \frac{di_2}{dt} - V_{c4} + V_{co} \quad (8)$$

$$V_{FC} = V_{co} \quad (9)$$

$$V_{c1} = L_1 \frac{di_1}{dt} \quad (10)$$

$$V_{c4} = L_2 \frac{di_2}{dt} \quad (11)$$

By applying the voltage–second balance principle to inductors L1 and L2, the output voltage for all three modes has been obtained:

$$L_1 : d_1(V_{c1}) + (d_2 - d_1)(V_{c1} - V_{c2} - V_{c4}) + (1 - d_2)V_{c1} = 0 \quad (12)$$

$$V_{pv} = V_{c1} \quad (13)$$

$$V_{c4} = \frac{V_{c1}}{d_2 - d_1} \quad (14)$$

$$L_2 : d_2(V_{FC}) + (1 - d_2)(V_{FC} + V_{C4} - V_o) = 0 \quad (15)$$

$$V_o = \frac{V_{FC}(d_2 - d_1) + V_{C1}(1 - d_2)}{(1 - d_2)(d_2 - d_1)} \quad (16)$$

2.2 Second Mode of Operation

In this case, the battery is in the discharging state and supplies the load along with the panel and the fuel cell. This case has 4 switching states as shown in Fig. 4(a) to Fig. 4(b).

State 1 [t0, t1]: In this case, the inductors L1 and L2 are charging.

State 2 [t1, t2]: The capacitor C2 and the inductors L1 and L2 are charged by VPV + VBattery + VFC.

State 3 [t2, t3]: The inductor L1 is discharging into the capacitor C4.

State 4 [t3, t4]: The diode D8 is on and the energy of the capacitor C4 and the inductor L2 is discharged into the output capacitor.

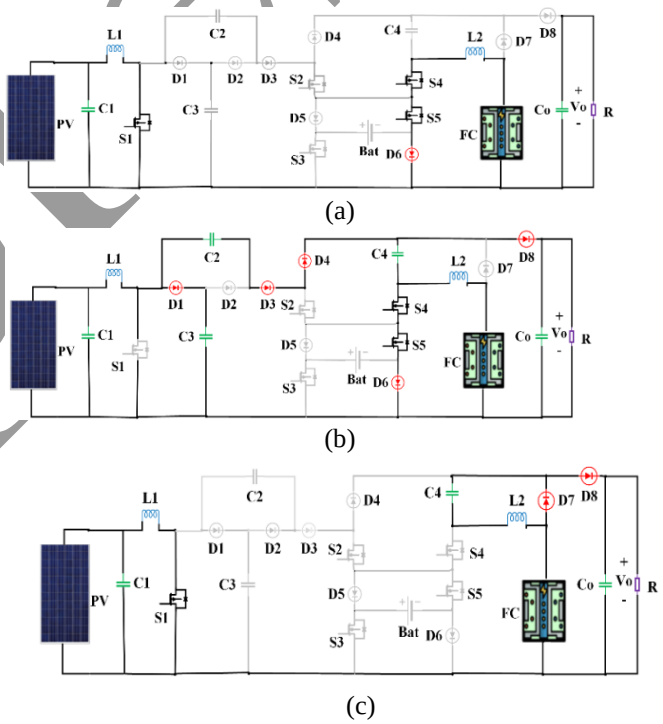
$$L_1 : d_1(V_{c1} + V_{battery}) + (d_2 - d_1)(V_{c1}) + \quad (17)$$
$$+(d_3 - d_2)(V_{c1} - V_{c4}) + (1 - d_3)(V_{c1}) = 0$$

$$V_{pv} = V_{c1} \quad (18)$$

$$V_{c4} = \frac{V_{c1} + d_1 V_{battery}}{d_3 - d_2} \quad (19)$$

$$L_2 : d_1(V_{FC} + V_{battery}) + (d_3 - d_1)(V_{FC}) + \quad (20)$$
$$+(1 - d_3)(V_{FC} + V_{c4} - V_o) = 0$$

$$V_o = \frac{(1 - d_3)(V_{c1} + d_1 V_{battery}) + (d_3 - d_2)(V_{FC} + d_1 V_{battery})}{(1 - d_3)(d_3 - d_2)} \quad (21)$$



(a)

(b)

(c)

Fig 3. First operation mode in state (a) 1, (b) 2, (c) 3.

2.3 Third Mode of Operation

The third mode occurs when the battery is charging and the load is powered by the panel and the fuel cell. The third mode of operation has 4 switching states, which are shown in Fig. 5(a) to Fig. 5(b).

State 1 [t0, t1]: In this case, the inductors L1 and L2 are charging.

State 2 [t1, t2]: The inductor L1 is charging the capacitor C4.

In process

State 3 [t2, t3]: The inductor L1 is charging with VC1-VBattery and the inductor L2 is charging with VFC-Vbattery.

State 4 [t3, t4]: In this case, switch S2 is on and inductor L1 is discharged with VC1-VBattery and inductor L2 with VFC-Vbattery and supplies the output load.

$$L_1 : d_1(V_{c1}) + (d_2 - d_1)(V_{c1} - V_{c4}) + \quad (22)$$
$$+(1-d_2)(V_{c1} - V_{battery}) = 0$$

$$V_{pv} = V_{c1} \quad (23)$$

$$V_{c4} = \frac{V_{c1} - (1-d_2)V_{battery}}{d_2 - d_1} \quad (24)$$

$$L_2 : d_2(V_{FC}) + (d_3 - d_2)(V_{FC} - V_{battery}) + \quad (25)$$
$$+(1-d_3)(V_{FC} + V_{c4} - V_o) = 0$$

$$V_o = \frac{(V_{FC} - (d_3 - d_2)V_{battery})}{(1-d_3)} + \frac{(V_{c1} - (1-d_2)V_{battery})}{(d_2 - d_1)} \quad (26)$$

The key waveforms of some converter elements under the three operating modes are shown in Fig. 6. The voltage gain of the proposed converter at different duty cycle values in mode 1 is shown in Fig. 7.

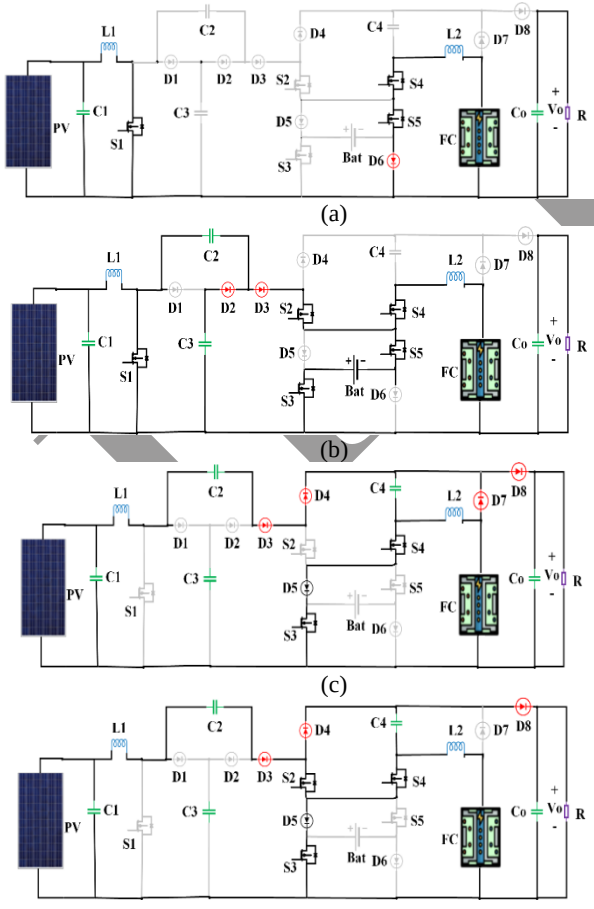


Fig 4. Second Operation mode in state (a) 1, (b) 2, (c) 3, (d) 4.

3 Converter Comparison

In this part, Table 2 compares the proposed converter with other similar articles. The comparison reveals that the suggested converter exhibits high efficiency and achieves a high voltage gain and is suitable for use in photovoltaic systems. The converter efficiency is obtained according to the procedure mentioned in [23]. In Fig. 8(a), the converter efficiency is plotted separately for each mode, and in Fig. 8(b), the percentage of losses for each section of the converter is presented.

Table 1. Status of semiconductor elements in each converter mode.

No. of mode	Sub-mode	Conditions	time interval	State Numbers
1	1	S1,S4,S5,D6=ON S2,S3,D1,D2,D3,D4, D5,D7,D8= OFF	[t0-t1]	1-1
	2	S4,S5,D1,D3,D4,D6,D8 =ON S1,S2,S3,D2,D5,D7 =OFF	[t1-t2]	1-2
	3	S1, D7, D8=ON S2,-S5, D1-D6 =OFF	[t2-t3]	1-3
2	1	S1,S4,S5,D6=ON S2,S3,D4,D5,D1,D7,D2,D3,D8 =OFF	[t0-t1]	2-1
	2	S1,-S5, ,D2, D3, D6=ON D1,D4,D5,D7,D8 =OFF	[t1-t2]	2-2
	3	S3,S4,D7,D3,D4,D5,D8 =ON S1,S2,S5,D1,D2,D6 =OFF	[t2-t3]	2-3
	4	S2,S3,S4, ,D3,D4, D5,D8=ON D1,D2,S1,S5,D6,D7 =OFF	[t3-t4]	2-4
3	1	S1,S4,S5, D6=ON S2,S3, D4,D3, D5,D1, D7,D2,D8 =OFF	[t0-t1]	3-1
	2	S3,S1,S4,D4,D2, D3, =ON S2,S5,D1,D6,D5,D7,D8 =OFF	[t1-t2]	3-2

Press

3	S2,S4,D3, D6,D5,D8,D7, =ON S3,S1,S5,D4,D2,D1 =OFF	[t2-t3]	3-3
4	S2,D3-D8 =ON S4,S3,S1,S5, D1,D2 =OFF	[t3-t4]	3-4

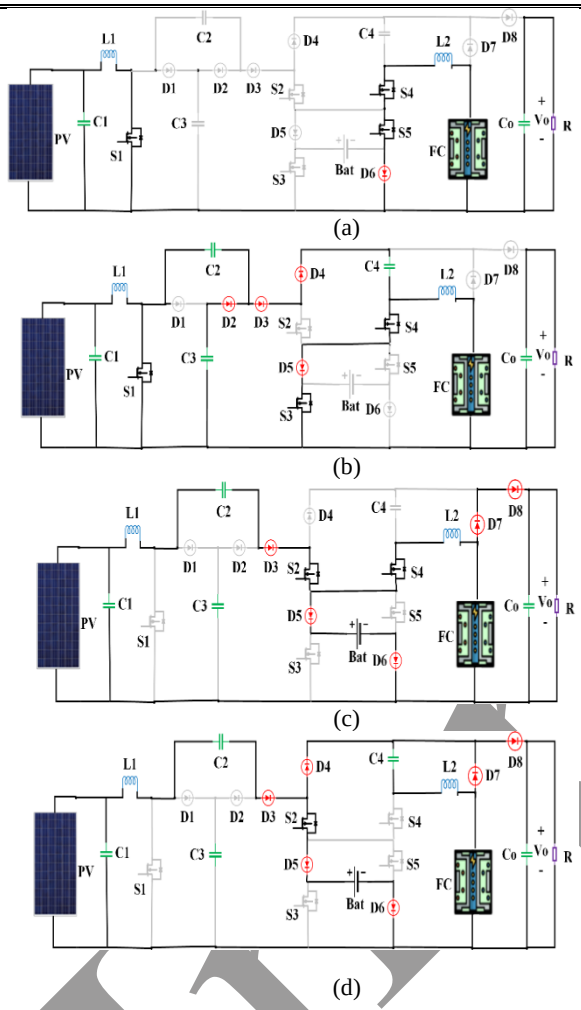
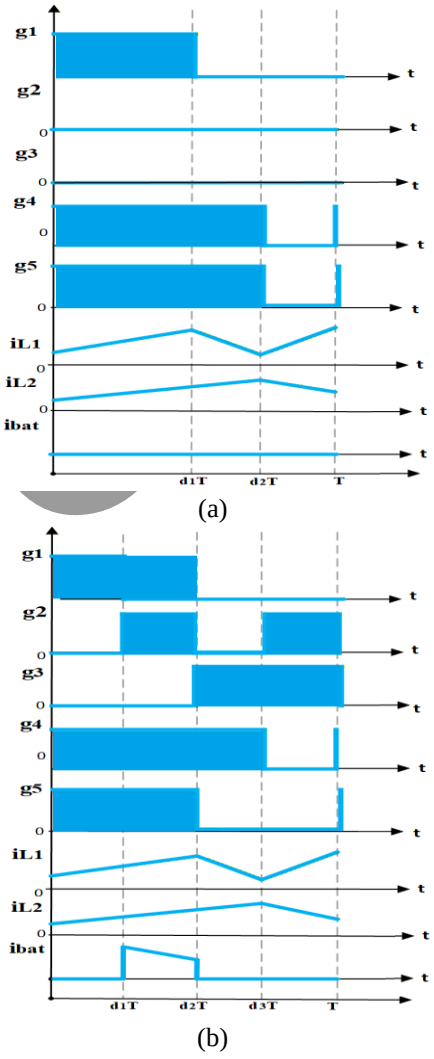


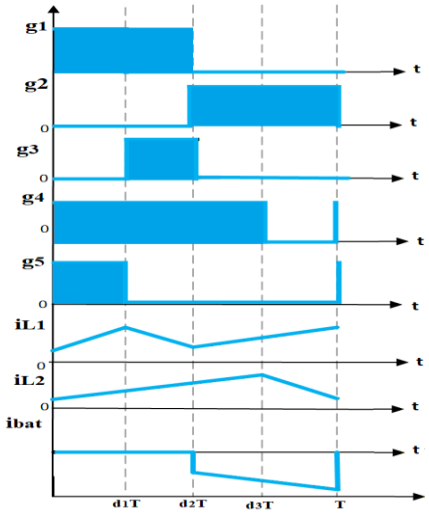
Fig 5. Third operation mode in case (a) 1, (b) 2, (c) 3, (d) 4.

Table 2. Comparison of converters.

Topology	Proposed converter	[24]	[25]	[26]	[27]
No. of inputs	3	2	3	3	3
No. of outputs	1	1	2	1	1
No. of Switches	5	5	4	4	4
No. of Inductors	2	1	4	2	2
High voltage gain	✓	×	✓	×	✓
Non-isolated	Yes	Yes	Yes	Yes	Yes
Efficiency	96-98%	92%	94.2%	95.8%	93%-96.5%



IJEEE



(c)

Fig 6. Waveforms for the converter (a)1 (b)2 (c)3.

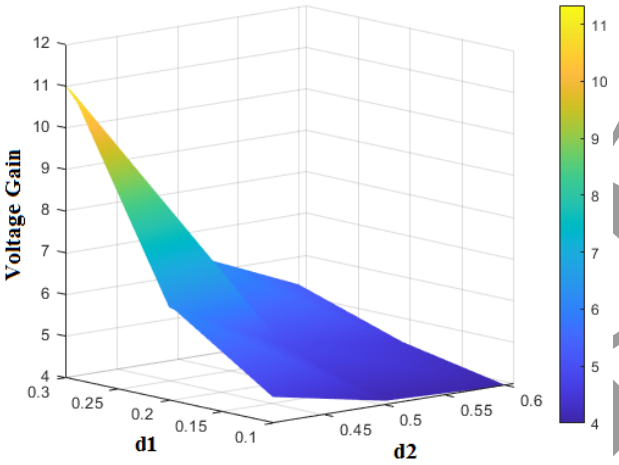
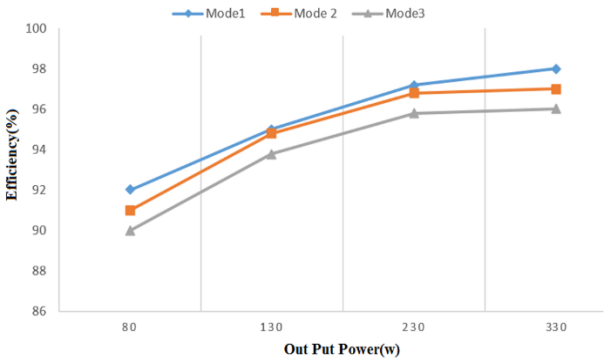


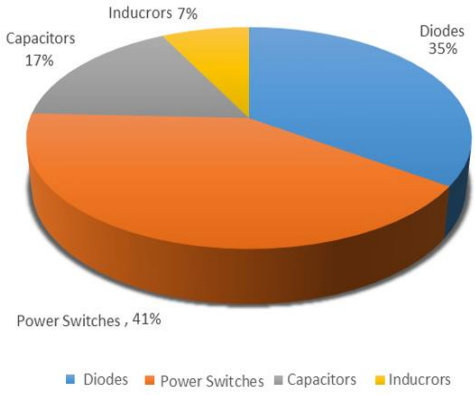
Fig 7. Voltage gain of the suggested converter.

4 Simulation Results

The performance of the suggested multi-input converter is evaluated using simulation in MATLAB software. The parameters of the converter are illustrated in Table 3. The proposed converter has an input port consisting of a 30 V solar panel, a 25 V fuel cell, and a 24 V lithium-ion battery. The simulation results for the converter are illustrated in Fig. 9(a) through Fig. 9(j).



(a)



(b)

Fig 8. (a) Converter efficiency (b) Percentage of losses for each element of the converter.

Table 3. Converter simulation specifications.

Parameter	Value
L1	2mH
L2	2uH
C1	1uF
C2	16uF
C3	16uF
C4	1mf
Co	10mF
fs	20KHz
Load R	30-80 (Ω)
Vo	160V
Vpv	30v
Vbattery	24v
Vfc	25
Pout	330w

Fig. 9(a) shows the output voltage alongside the two input voltages. As can be seen, the output voltage is correctly regulated at 160 V and reaches its steady-state value in approximately 0.25 seconds, while the input voltages remain constant at their nominal values (30 V for VPV and 25 V for VFC).

This demonstrates effective voltage regulation. Fig. 9(b) illustrates the voltage across diode VD2, demonstrating the diode's proper operation. Fig. 9(c) and

Fig. 9(d) show the constant voltages of the PV and the fuel cell, respectively.

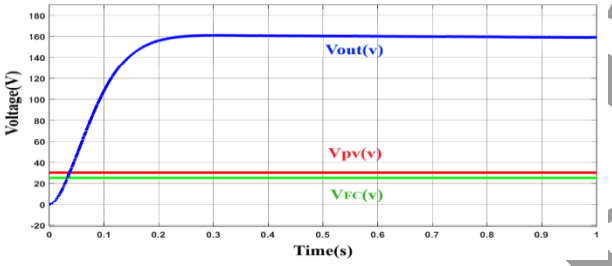
Fig. 9(e) and Fig. 9(f) display the gate signals for S2 and S4, confirming the desired duty-cycle operation of the switches. Fig. 9(g) shows the output current (Io) stabilizing at 2.06 A—a value corresponding to an output power of 330 W at a voltage of 160 V.

Fig. 9(h) displays the output voltage and confirms its regulation at 160 V, as previously observed in Fig. 9(a).

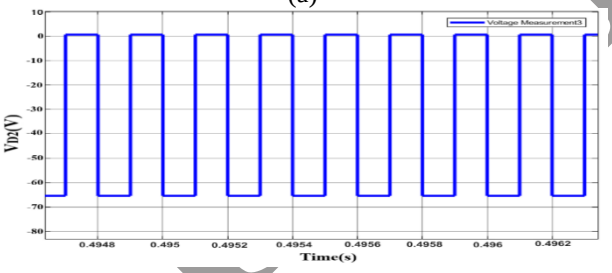
Fig. 9(i) shows the output power (Po), which stabilizes at approximately 330 W, aligning with the design specifications. The gradual rise and stable steady-state operation indicate satisfactory power transfer from the input sources to the load. Fig. 9(j) displays the battery voltage throughout the simulation.

Following a brief initial transient period resulting from charge/discharge dynamics, the battery voltage stabilizes at approximately 24 V, demonstrating stable bidirectional power management between the battery and the other sources.

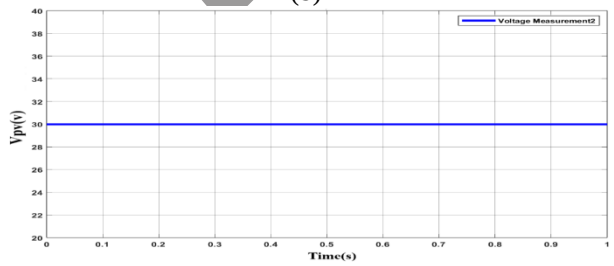
Overall, the results in Fig. 9 confirm proper voltage regulation and stable operation of the proposed converter under nominal operating conditions.



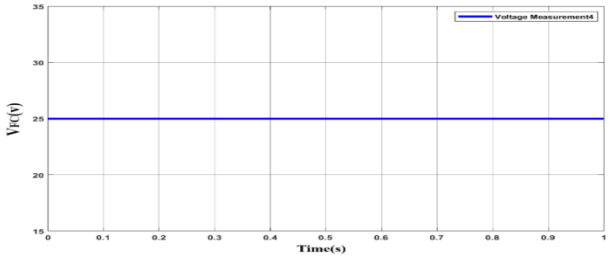
(a)



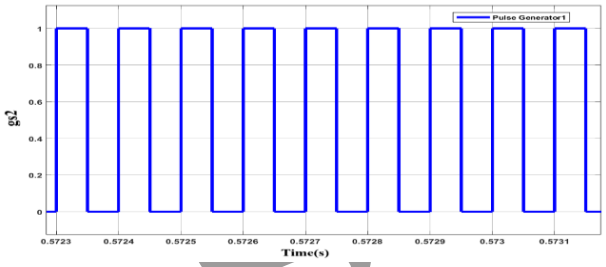
(b)



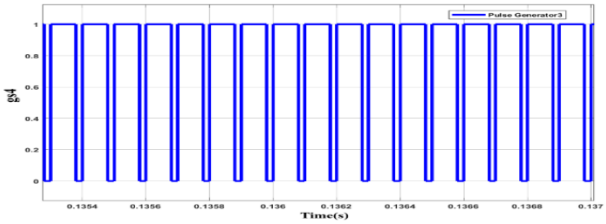
(c)



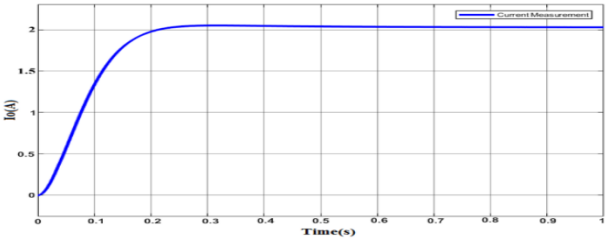
(d)



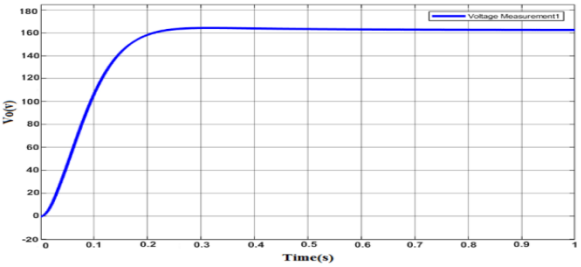
(e)



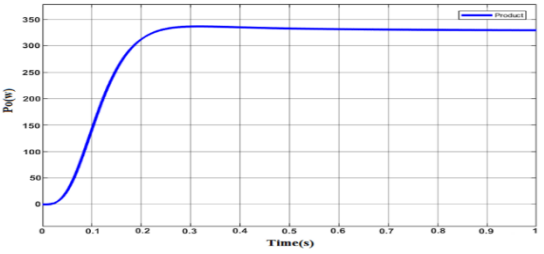
(f)



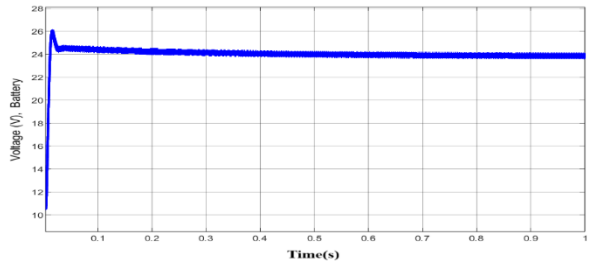
(g)



(h)



(i)



(j)

Fig 9. The converter simulation results in mode1:(a) Voltage of input – output converter, (b) V_{D2}, in mode 3 (c) V_{pv} (d) V_{fc}, (e) V_{gs2}, (f) V_{gs4}, (g)I_{out}, (h) V_o, (i) P_{out}, (j) $V_{battery}$.

5 Conclusion

In this study, a new MI DC-DC converter is presented for the integrated connection of photovoltaic, fuel cell, and battery sources. By reducing the component count, eliminating the bulky transformer, lowering input current ripple, and utilizing a common ground, the proposed topology offers a suitable solution for applications where source current quality, reliability, and system integration are critical. To validate the theoretical analyses, a 330 W converter was simulated in MATLAB/Simulink. The results demonstrate effective regulation of the 160 V output voltage and satisfactory power transfer among the input sources under various operating conditions. An efficiency exceeding 95% across all three operating modes at 330 W confirms the feasibility and satisfactory performance of the proposed converter within the investigated range. Overall, the results indicate that the proposed topology can serve as an integrated stage for hybrid photovoltaic/fuel cell/battery systems, thereby reducing the need for multiple separate converters.

Nomenclature

d	Duty cycle
MI	Multi Input
PV	Photovoltaic
V_{c1}	Capacitor voltage C_1
V_{c4}	Capacitor voltage C_4
V_{fc}	Fuel cell voltage
V_{pv}	Solar panel voltage
$V_{battery}$	Battery voltage
V_o	Output voltage

Conflict of Interest

The authors declare no conflict of interest.

Author Contributions

Homa Zarei Zohdi: Conceptualization; Data curation; Methodology; Software; Validation; Visualization; Writing – original draft.

Mohammad Sarvi: Supervision; Writing – review and editing.

Heidar Ali Shayanfar: Supervision; Writing – review and editing. All authors have read and agreed to the published version of the manuscript.

Funding

No funding was received for this work.

Declaration of generative AI and AI-assisted technologies

The authors declare that no generative AI or AI-assisted technologies were used in the writing process of this manuscript.

Acknowledgment

The authors wish to thank A, B, C. This work was supported in part by a grant from XYZ.

References

[1] Dada M, Popoola P. Recent advances in solar photovoltaic materials and systems for energy storage applications: a review. Beni-Suef Univ J Basic Appl Sci 2023;12:66. https://doi.org/10.1186/s43088-023-00405-5.

[2] Iturralde Carrera LA, Garcia-Barajas MG, Constantino-Robles CD, Álvarez-Alvarado JM, Castillo-Alvarez Y, Rodríguez-Reséndiz J. Efficiency and Sustainability in Solar Photovoltaic Systems: A Review of Key Factors and Innovative Technologies. Eng 2025;6:50. https://doi.org/10.3390/eng6030050.

[3] Enasel E, Dumitrascu G. Storage solutions for renewable energy: A review. Energy Nexus 2025;17:100391. https://doi.org/10.1016/j.nexus.2025.100391.

[4] Olabi AG, Elsaid K, Obaideen K, Abdelkareem MA, Rezk H, Wilberforce T, et al. Renewable energy systems: Comparisons, challenges and barriers, sustainability indicators, and the contribution to UN sustainable development goals. Int J Thermofluids 2023;20:100498. https://doi.org/10.1016/j.ijft.2023.100498.

[5] Zarei Zohdi H, Sarvi M. Analysis and Design of a New DC-DC Converter for DC Smart Grid. J Sol Energy Res n.d.;8:1547–58. https://doi.org/10.22059/jser.2023.357223.1290.

[6] Yildirim B, Elgendy MA, Smith A, Kulan MC, Akbal B. Modular-Multi-Port-Converter-Based

In press

Battery Energy Storage System with Integrated Battery Management Functions. Energies 2025;18:3142. https://doi.org/10.3390/en18123142.

[7] N. K, M. R, M. V, Aldosari O. Experimentation of Multi-Input Single-Output Z-Source Isolated DC–DC Converter-Fed Grid-Connected Inverter with Sliding Mode Controller. Sustainability 2023;15:16875. https://doi.org/10.3390/su152416875.

[8] Behjati H, Davoudi A. Single-stage multi-port DC–DC converter topology. IET Power Electron 2013;6:392–403. https://doi.org/10.1049/iet-pel.2012.0339.

[9] Imanlou A, Babaei E, Hosseini SH. A New High Voltage Gain Common-Ground Step-Up DC-DC Converter Integrating Coupled-Inductors and Switched-Capacitors. Int J Circuit Theory Appl 2025;53:5394–409. https://doi.org/10.1002/cta.4342.

[10] Ebrahimnaz R, Sarvi M, Zohdi HZ. A High-Gain Converter for Electric Vehicle Application. 2024 4th Int. Conf. Electr. Mach. Drives, IEEE; 2024, p. 1–6. https://doi.org/10.1109/ICEMD64575.2024.10963422.

[11] Askarian I, Pahlevani M, Knight AM. Three-Port Bidirectional DC/DC Converter for DC Nanogrids. IEEE Trans Power Electron 2021;36:8000–11. https://doi.org/10.1109/TPEL.2020.3046453.

[12] Chen YM, Huang AQ, Yu X. A high step-up three-port DC-DC converter for stand-alone PV/battery power systems. IEEE Trans Power Electron 2013;28:5049–62. https://doi.org/10.1109/TPEL.2013.2242491.

[13] KhademiAstaneh P, Javidan J, Valipour K, Akbarimajd A. A bidirectional high step-up multi-input DC-DC converter with soft switching. Int Trans Electr Energy Syst 2019;29:e2699. https://doi.org/10.1002/etep.2699.

[14] Shen C-L, Chen L-Z. Dual-Input Isolated Converter With Dual-Charge-Pump Cell for High Step-Up Voltage Ratio Achievement. IEEE Trans Ind Electron 2020;67:9383–92. https://doi.org/10.1109/TIE.2019.2952793.

[15] Subramanian A, Karuppiah S. Analysis of dual-input three-port isolated DC–DC converter with bidirectional capability. J Power Electron 2022;22:711–26. https://doi.org/10.1007/s43236-022-00408-y.

[16] Chandran IR, Ramasamy S, Ahsan M, Haider J, Rodrigues EMG. Implementation of Non-Isolated Zeta-KY Triple Port Converter for Renewable Energy Applications. Electronics 2021;10:1681. https://doi.org/10.3390/electronics10141681.

[17] Cheng T, Lu DD-C, Qin L. Non-Isolated Single-Inductor DC/DC Converter With Fully Reconfigurable Structure for Renewable Energy Applications. IEEE Trans Circuits Syst II Express Briefs 2018;65:351–5. https://doi.org/10.1109/TCSII.2017.2712286.

[18] Gulhane AP, Khamankar M, Dhoble S, Thakre T, Katekhaye T, Khubalkar S. Multiport DC-DC Converter for Efficient Power Distribution in Diverse Applications. 2024 Int. Conf. Sustain. Power & Energy, IEEE; 2024, p. 1–6. https://doi.org/10.1109/ICSPE62629.2024.10924351.

[19] Farajdadian S, Hajizadeh A, Soltani M. Recent developments of multiport DC/DC converter topologies, control strategies, and applications: A comparative review and analysis. Energy Reports 2024;11:1019–52. https://doi.org/10.1016/j.egyr.2023.12.054.

[20] Harrison S, Soltoswski B, Pepiciello A, Camilo Henao A, Farag AY, Beza M, et al. Review of multiport power converters for distribution network applications. Renew Sustain Energy Rev 2024;203:114742. https://doi.org/https://doi.org/10.1016/j.rser.2024.114742.

[21] Jalilzadeh T, Rostami N. A new bidirectional multi-port DC-DC converter suitable for hybrid energy systems: design, analysis, and implementation. Electr Eng 2025;107:14099–119. https://doi.org/10.1007/s00202-025-03254-w.

[22] Muñoz-Peña P, Cheah-Mane M, Gomis-Bellmunt O, Prieto-Araujo E. Multiport converter evaluation for high penetration of renewable generation in distribution grids. Int J Electr Power Energy Syst 2024;161:110211. https://doi.org/10.1016/j.ijepes.2024.110211.

[23] Glitz ES, Ordonez M. MOSFET Power Loss Estimation in LLC Resonant Converters: Time Interval Analysis. IEEE Trans Power Electron 2019;34:11964–80. https://doi.org/10.1109/TPEL.2019.2909903.

[24] Naeiji S, Abdollahi SE, Abdollahi SR, Baigzadehnoe B. An Improved Bidirectional Non-Isolated Dual-Input DC-DC Converter for Electric Vehicles Application. 2023 14th Power Electron. Drive Syst. Technol. Conf., IEEE; 2023, p. 1–7. https://doi.org/10.1109/PEDSTC57673.2023.10087176.

[25] S. Rostami, V. Abbasi and NT. Ultrahigh step-up multiport DC-DC converter with common grounded input ports and continuous input

In Press

current. IEEE Trans Ind Electron 2021;69:12859–73.
[26] Aravind R, Chokkalingam B, Verma R, Aruchamy S, Mihet-Popa L. Multi-Port Non-Isolated DC-DC Converters and Their Control Techniques for the Applications of Renewable Energy. IEEE Access 2024;12:88458–91. https://doi.org/10.1109/ACCESS.2024.3413354.
[27] Rostami S, Abbasi V, Parastesh M. Design and Implementation of a Multiport Converter Using Z-Source Converter. IEEE Trans Ind Electron 2021;68:9731–41. https://doi.org/10.1109/TIE.2020.3022538.

Biographies (All Authors)



Homa Zarei Zohdi received the M.Sc. degree in electrical engineering from Imam Khomeini International University, Qazvin, Iran, in 2023. She is currently pursuing the Ph.D. degree in School of Electrical Engineering, Iran University of Science and Technology. Her research interests include the design and performance analysis of power electronic converters.



Mohammad Sarvi received the M.Sc. and Ph.D. degrees in electrical engineering from Iran University of Science and Technology, Tehran, Iran, in 1999 and 2004, respectively. He is currently an Associate Professor with the School of Electrical Engineering, Iran University of Science and Technology.



Heidar Ali Shayanfar received the B.S. and M.S.E. degrees in electrical engineering in 1973 and 1979, respectively. He received the Ph.D. degree in electrical engineering from Michigan State University, East Lansing, MI, USA, in 1981. Currently, he is a full professor with the Department of Electrical Engineering, Iran University of Science and Technology, Tehran, Iran. His research interests are in the application of artificial intelligence to power system control design, dynamic load modeling, power system observability studies, voltage collapse, and congestion management in a restructured power system, reliability improvement in distribution systems, smart grids and reactive pricing in deregulated power systems. He has published more than 750 technical papers in the international journals and conferences proceedings. Dr. Shayanfar is a member of the Iranian Association of Electrical and Electronic Engineers.

In press